Supplementary Materials for the Paper Entitled "Reducing Scaling Effect on Downscaled Land Surface Temperature Maps in Heterogenous Urban Environments"

Ruiliang Pu [1] and Stefania Bonafoni [2]
[1]School of Geosciences, University of South Florida, Tampa, FL 33620 USA, Email: rpu@usf.edu; Phone: +1 813 974 1508
[2]Department of Engineering, University of Perugia, 06125 Perugia, Italy, Email: stefania.bonafoni@unipg.it; phone: +39 075 585 3663.

S1: DLST maps created from ASTER 90 m LST with CASE I data set

Figure S1 presents the scatter plots in a two-dimension feature space (difference (D_{iff}LST) between ULSTs and DLSTs and the combined SD of red and NIR bands) to show the triangle-shape pattern of the scattered points with CASE I data set. Plots (a – e) were created with 54 m, 46 m, 38 m, 22 m, and 10 m resolution map data.

Figure S2 shows the corrected DLST maps downscaled from ASTER 90 m LST with AISA data derived spectral clusters and the modified TSU model. Plots (a1 – e1) are 54 m, 46 m, 38 m, 22 m, and 10 m DLST maps, and plots (a2 – e2) are the corresponding reference LST maps (ULST) upscaled from the TABI 2 m LST map. By checking and comparing the corrected DLST results and the corresponding ULSTs, it is clearly observed that spatial distribution patterns and locations of LSTs were well consistent.

In Figure S3, scatter plots between DLSTs (a1 – e1) and corrected DLSTs (a2 – e2) with the CT expression (Y = – 0.25 • X+ 320), and corresponding ULST aggregated from the TABI 2 m LST (*i.e.*, reference map), are reported. The DLST results were created from ASTER 90 m LST with AISA data derived 10 spectral clusters and by the modified TSU model. Results suggested that using CT to reduce the scaling effect on DLST maps is workable and effective, especially at very high resolutions.

Table S1 summarizes the RMSE and MAE values for DLST (W/out CT in the table) and corrected DLST maps, as well as the DLST accuracy improvement after DLST maps were corrected with the same CT expression (*i.e.*, Y = 0.25 • X+ 320) for CASE I, by using the REG model. Per the table, it is apparent that after correction, the RMSE and MAE errors were significantly reduced at different resolutions (*i.e.*, the accuracy of DLST maps were significantly increased). The average RMSE value across 6 m to 62 m resolutions was reduced 40%, and the average MAE value 45% in CASE I study area.

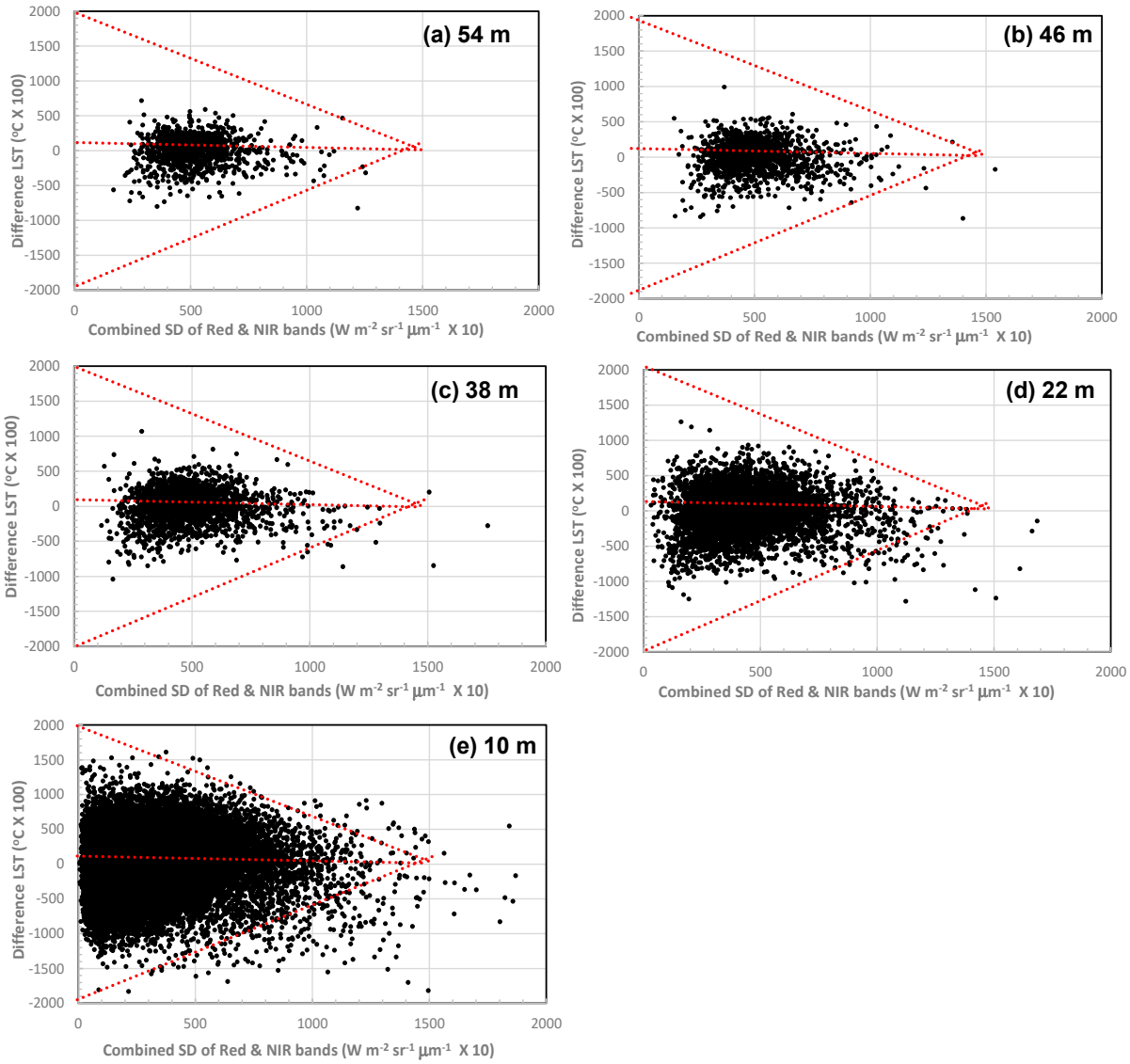

Figure S1. Scatter plots in a two-dimension feature space of the difference (D_{iff}LST) between ULSTs and DLSTs and the combined SD of red and NIR bands to present a triangle-shape pattern of the scattered points with CASE I data set. Plots (**a**–**e**) were created with 54 m, 46 m, 38 m, 22 m, and 10 m resolution map data.

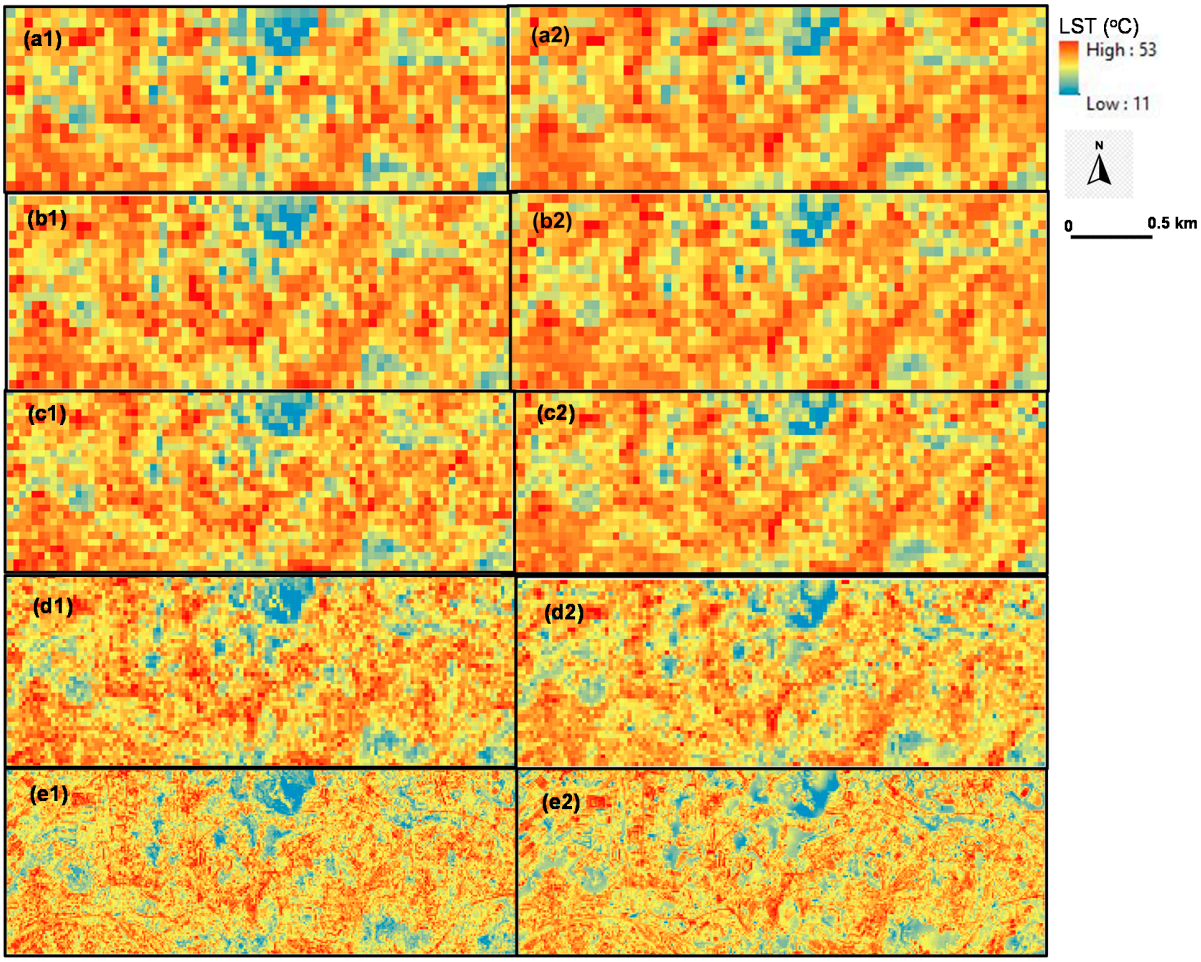

Figure S2. Corrected DLST maps downscaled from ASTER 90 m LST with AISA data derived spectral clusters by applying the modified TSU model. (**a1**–**e1**) are 54 m, 46 m, 38 m, 22 m, and 10 m DLST maps, and (**a2**–**e2**) are the corresponding reference LST maps (ULST) upscaled from the TABI 2 m LST map.

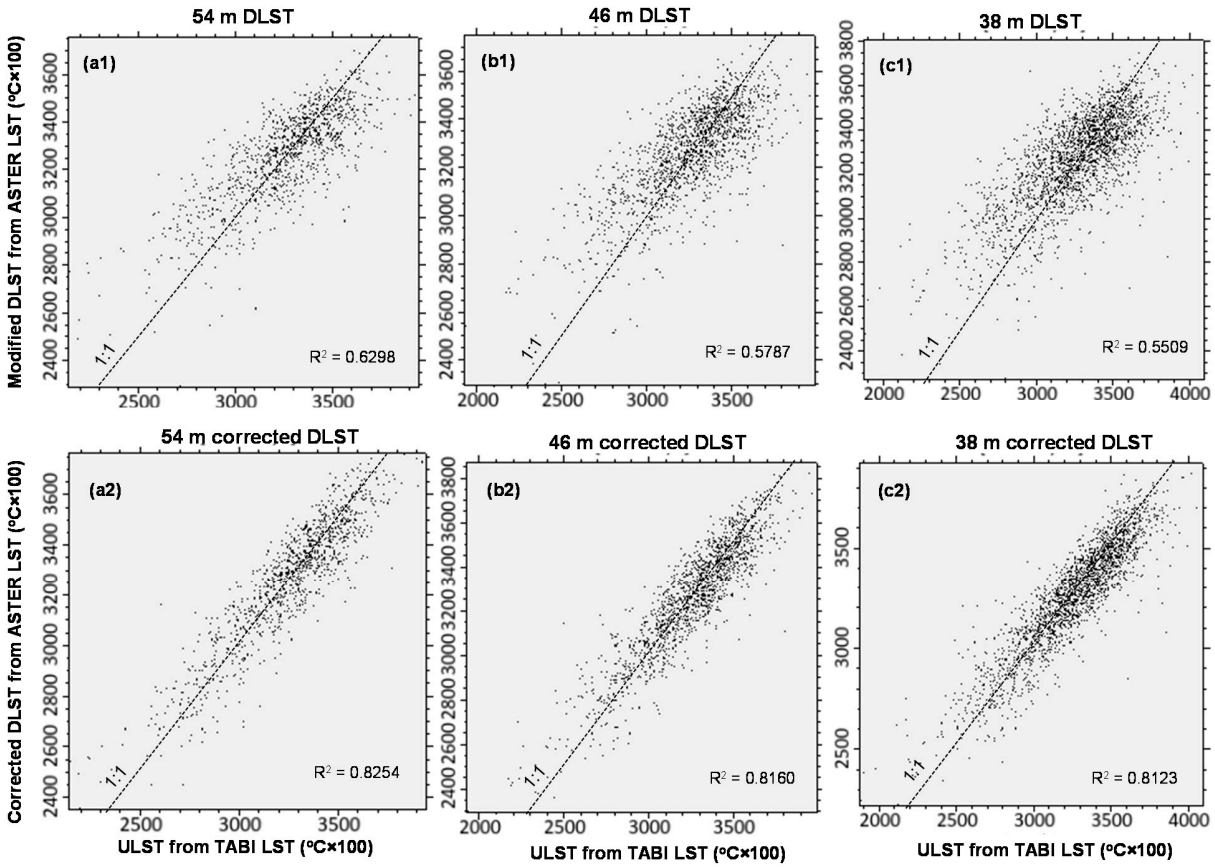
54 m DLST
46 m DLST
38 m DLST
(a1)
(b1)
(c1)
Modified DLST from ASTER LST (°C×100)
1:1
R² = 0.6298
R² = 0.5787
R² = 0.5509
54 m corrected DLST
46 m corrected DLST
38 m corrected DLST
(a2)
(b2)
(c2)
Corrected DLST from ASTER LST (°C×100)
R² = 0.8254
R² = 0.8160
R² = 0.8123
ULST from TABI LST (°C×100)
ULST from TABI LST (°C×100)
ULST from TABI LST (°C×100)

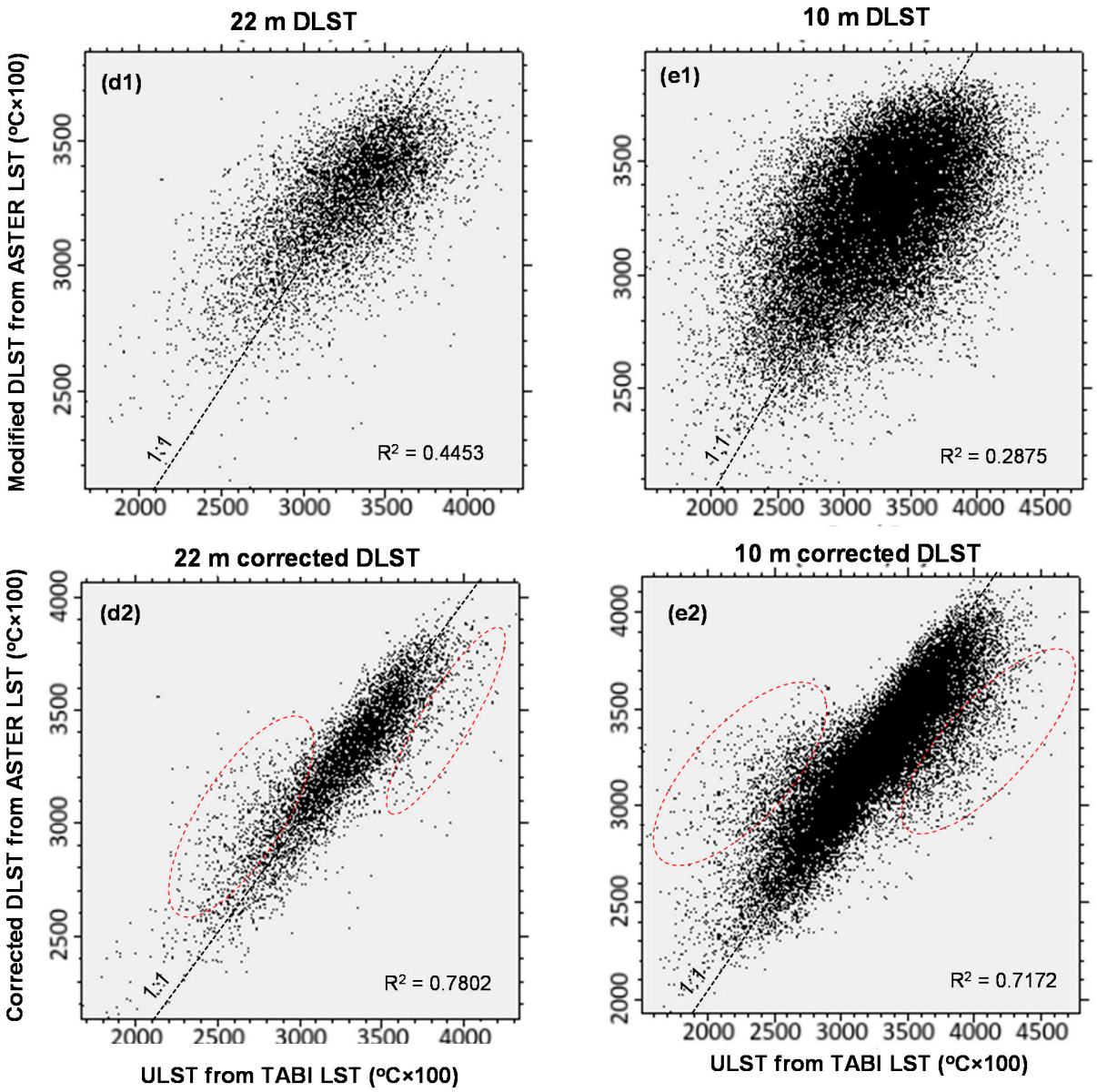

Figure S3. Scatter plots (CASE I) between DLST results (**a1**–**e1**) and corrected DLST results (**a2**–**e2**) with the CT expression (Y = – 0.25 • X+ 320), and corresponding ULST aggregated from the TABI 2 m LST.The DLST results were created from ASTER 90 m LST with AISA data derived 10 spectral clusters and by applying the modified TSU model.

Table S1. Summary of RMSE and MAE values improved with correction term (CT) to correct DLSTs for CASEs I and II data sets

DLST	RMSE (^{0}C)			MAE(^{0}C)			Note
	W/out CT	With CT	Improved With CT(%)	W/out CT	With CT	Improved With CT(%)	
CASE I with ASTER 90 m LST and AISA optical data (DLST by using the REG model)							
60 m DLST	1.06	0.79	25.47	0.82	0.63	23.17	compared to ULST of TABI 2m LST
45 m DLST	1.46	0.85	41.78	1.14	0.65	42.98	compared to ULST of TABI 2m LST
30 m DLST	1.99	1.11	44.22	1.53	0.77	49.67	compared to ULST of TABI 2m LST
20 m DLST	2.49	1.43	42.57	1.91	0.95	50.26	compared to ULST of TABI 2m LST
15 m DLST	2.88	1.65	42.71	2.22	1.08	51.35	compared to ULST of TABI 2m LST
10 m DLST	3.41	2.01	41.06	2.66	1.32	50.38	compared to ULST of TABI 2m LST
6 m DLST	3.99	2.36	40.85	3.16	1.57	50.32	compared to ULST of TABI 2m LST
Average			**39.81**			**45.45**	
CASE II with high resolution thermal retrieved LST and optical data (DLST by using the modified TC-based TSU model)							
62 m DLST	1.88	1.37	27.13	1.26	0.92	26.98	compared to ULST of retrieved 2m LST
54 m DLST	1.80	1.30	27.78	1.23	0.88	28.46	compared to ULST of retrieved 2m LST
46 m DLST	1.98	1.39	29.80	1.32	0.95	28.03	compared to ULST of retrieved 2m LST
38 m DLST	2.21	1.57	28.96	1.49	1.03	30.87	compared to ULST of retrieved 2m LST
30 m DLST	2.41	1.69	29.88	1.63	1.08	33.74	compared to ULST of retrieved 2m LST
22 m DLST	2.68	1.86	30.60	1.80	1.16	35.56	compared to ULST of retrieved 2m LST
14 m DLST	3.07	2.13	30.62	2.07	1.31	36.71	compared to ULST of retrieved 2m LST
10 m DLST	3.35	2.31	31.04	2.27	1.40	38.33	compared to ULST of retrieved 2m LST
6 m DLST	3.78	2.65	29.89	2.58	1.57	39.15	compared to ULST of retrieved 2m LST
Average			**29.52**			**33.09**	

S2: DLST maps estimated from 100 m upscaled LST with CASE II data set

Figure S4 presents the scatter plots in a two-dimension feature space (difference (D_{iff}LST) between ULSTs and DLSTs and the combined SD of red and NIR bands) to show the triangle-shape pattern of the scattered points. Plots (a – d) were created with 62 m, 30 m, 14 m, and 6 m resolution with CASE II data set. The remaining 54 m, 46 m, 38 m, 22 m, and 10 m plots have a similar triangle-shape pattern as Figure S4.

Figure S5 shows the scatter plots between DLST results (a1 – d1) and corrected DLST results (a2 – d2) with the CT expression (Y = – 0.25 • X+ 320), and corresponding ULST aggregated from the 2 m LST (*i.e.*, reference map). The DLST results were created from the 100 m upscaled retrieved LST with airborne multispectral data derived six scaling factors and the REG model. The remaining 54 m, 46 m, 38 m, 22 m, and 10 m LST scatter point plots have similar differences between DLSTs and corrected DLSTs. By checking the R^2 values of DLSTs and corrected DLSTs for corresponding resolutions, R^2 values after correction with CT model were significantly increased (R^2 value for corrected DLSTs increased from 0.25 for 62 m to 0.35 for 6 m with respect to the DLST maps). The results suggested that the CT correction term used for reducing the scaling effect on DLST maps is workable and effective also for CASE II.

Table S1 summarizes the RMSE and MAE values for DLST (W/out CT in the table) and corrected DLST maps, as well as the DLST accuracy improvement after DLST maps were corrected with the same CT expression (i.e., Y = 0.25 • X+ 320) for CASE II, by using the modified TSU model. Per the table, it is apparent that after correction, the RMSE and MAE errors were significantly reduced at different resolutions. The average RMSE value across 6 m to 62 m resolutions was reduced 30%, and the average MAE value 33% in CASE II study area.

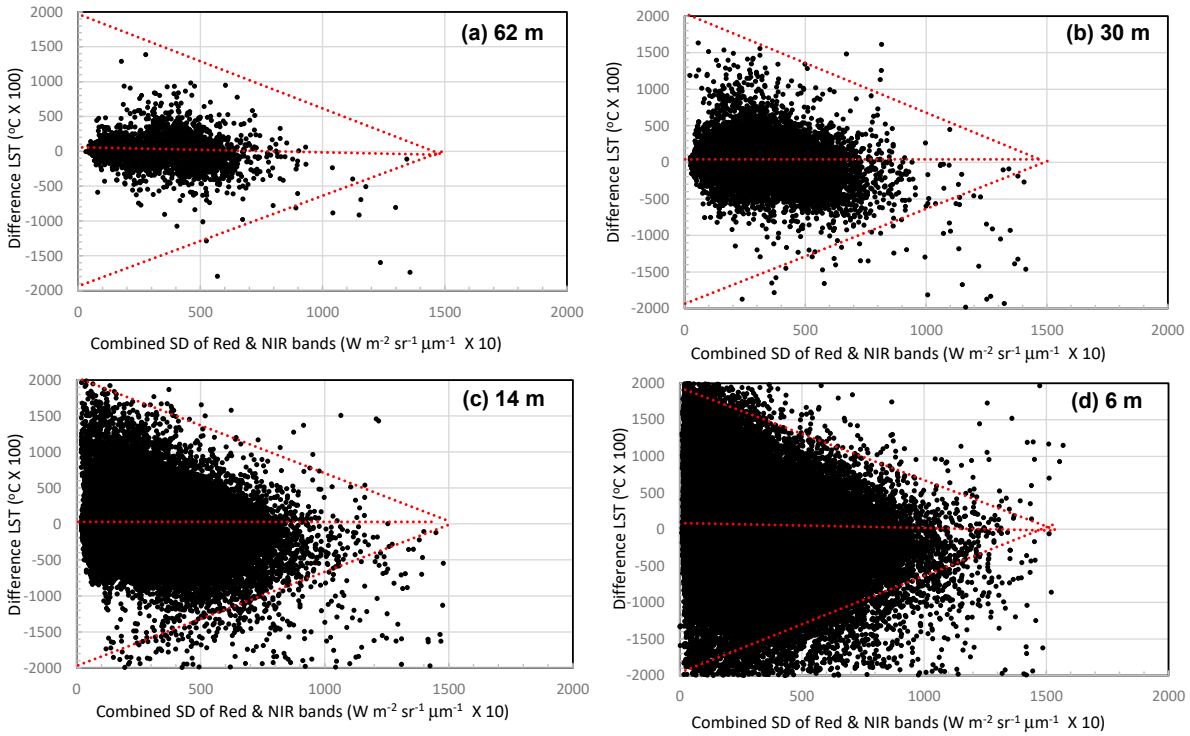

Figure S4. Scatter plots in a two-dimension feature space of the difference ($D_{iff}LST$) between ULSTs and DLSTs and the combined SD of red and NIR bands. Plots (**a**–**d**) were created with 62 m, 30 m, 14 m, and 6 m resolution map data with CASE II data set and the REG model. The remaining 54 m, 46 m, 38 m, 22 m, and 10 m plots have a similar triangle-shape pattern.

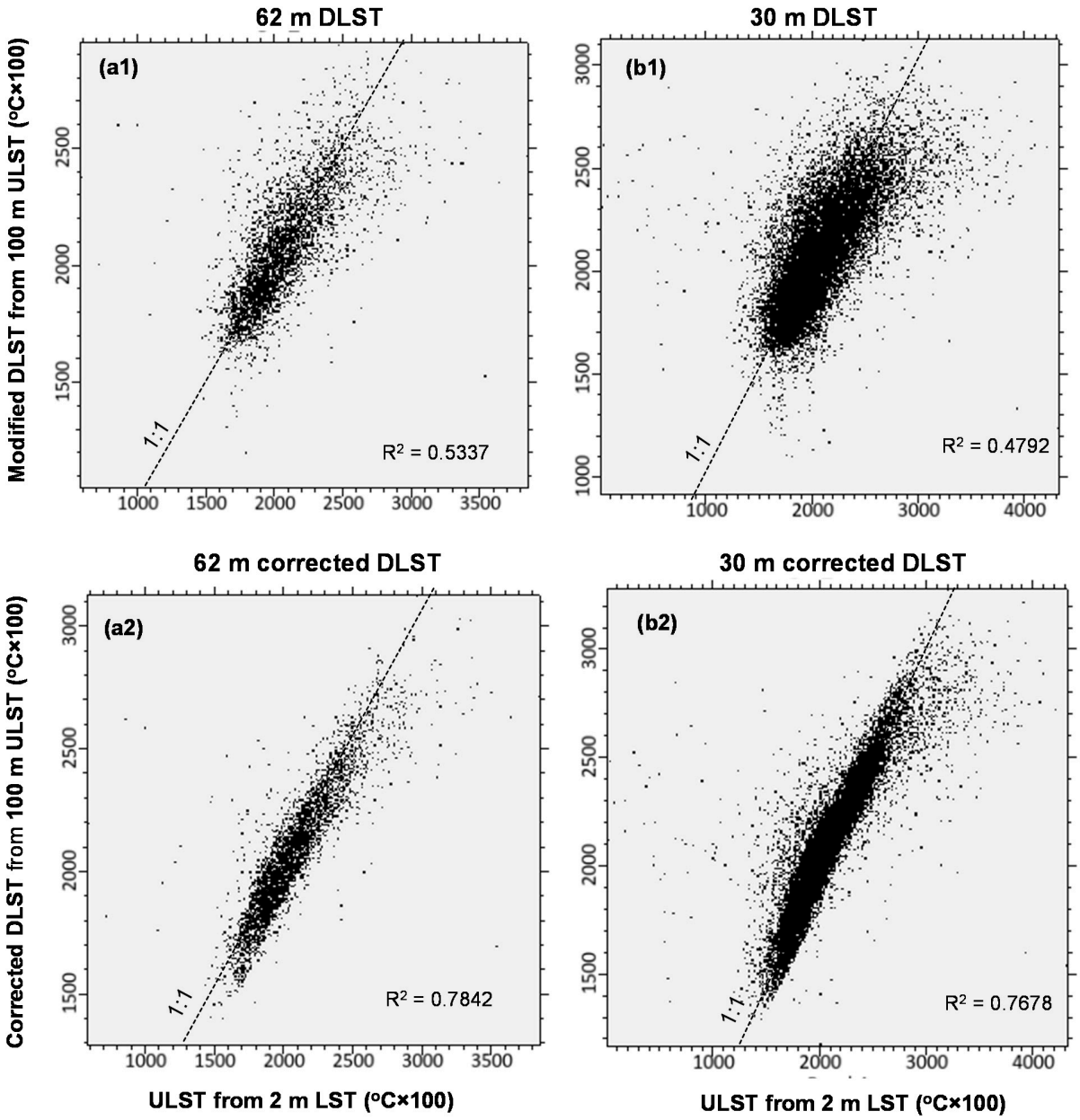
62 m DLST
30 m DLST
(a1)
(b1)
Modified DLST from 100 m ULST (°C×100)
1:1
R² = 0.5337
R² = 0.4792
62 m corrected DLST
30 m corrected DLST
(a2)
(b2)
Corrected DLST from 100 m ULST (°C×100)
R² = 0.7842
R² = 0.7678
ULST from 2 m LST (°C×100)
ULST from 2 m LST (°C×100)

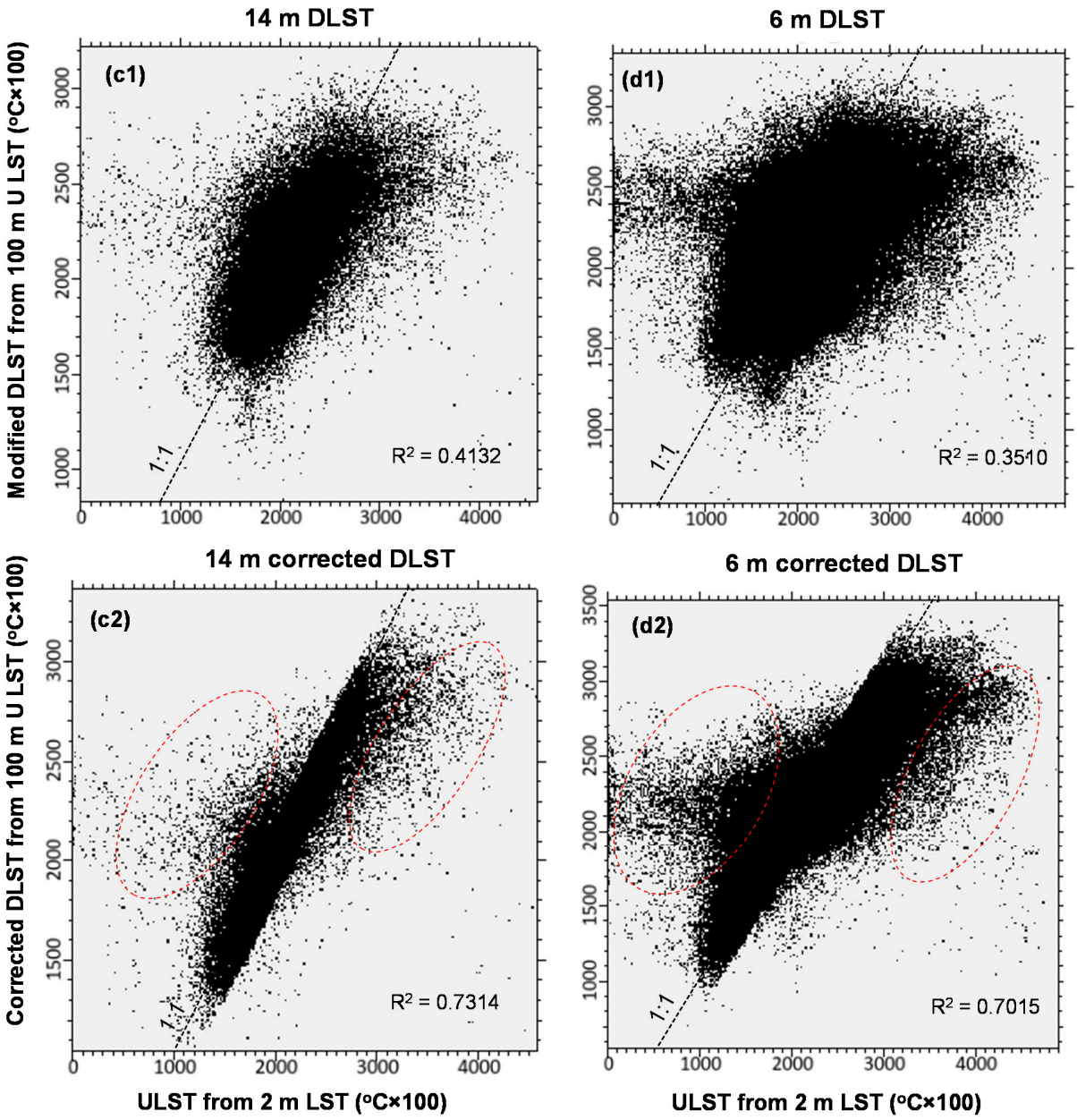

Figure S5. Scatter plots (CASE II) between DLST results (**a1**–**d1**) and corrected DLST results (**a2**–**d2**) with the CT expression (Y = – 0.25 • X+ 320), and corresponding ULST aggregated from the 2 m retrieved LST (i.e., reference map). The DLST results were created from the 100 m upscaled retrieved LST with airborne multispectral data derived six scaling factors and the REG model.